Trajectory Shift in Propagation of Electron Cyclotron Waves Due to Berry Curvature in Magnetized Plasma*)

Toru I. TSUJIMURA, Kota YANAGIHARA[1)], Yuki GOTO and Shin KUBO

National Institute for Fusion Science, National Institutes of Natural Sciences, Toki 509-5292, Japan
[1)]*National Institutes for Quantum and Radiological Science and Technology, Naka 311-0193, Japan*

(Received 15 November 2020 / Accepted 24 December 2020)

The polarization-dependent Hall effect of light was investigated in full-wave simulations for propagation of electron cyclotron waves in magnetized plasma as an anisotropic medium. The transverse shift of the wave packet, which is comparable to the wavelength in the vacuum, was observed in propagation of extraordinary (X) waves under a static magnetic field. This transverse shift is produced by the Berry curvature for the X wave strongly enhanced at the right-hand cutoff. The direction of the transverse shift is perpendicular not only to the gradient of the refractive index but also to the static magnetic field.

Keywords: electron cyclotron wave, Berry curvature, polarization-dependent Hall effect of light, full-wave simulation, propagation, transverse shift

DOI: 10.1585/pfr.16.2401009

1. Introduction

It is known that polarization of light affects propagation, shifting the wave path to the direction perpendicular to the gradient of the refractive index of media [1]. This effect gives deviation from the Snell's law in optics. The transverse shift of the wave-packet motion, referred to as the polarization-dependent spin Hall effect of light, is caused by the Berry phase [2] that originates from the spin angular momentum. When one considers the wave packet with a finite width of distribution such as a Gaussian beam, the Berry connection is obtained with the relative phase difference of the wave function in momentum ($\boldsymbol{k}$) space. This is analogous to a magnetic vector potential in real space. As is the case with a magnetic field obtained from rotation of the vector potential in real space, the Berry curvature is obtained from rotation of the Berry connection in $\boldsymbol{k}$ space. The "force" by the Berry curvature, analogous to the Lorentz force by a magnetic field in real space, gives rise to the transverse shift in "real" space.

From [1], the Berry curvature $\boldsymbol{\Omega}$ of light propagating in isotropic media is written as

$$\boldsymbol{\Omega}(\boldsymbol{k}) = \sigma \frac{\boldsymbol{k}}{k^3}, \tag{1}$$

where σ is the spin angular momentum. $\sigma = \pm 1$ denotes the right-handed or left-handed circular polarizations. σ of an arbitrary elliptical polarization can be obtained by the linear combination of the two circular polarizations. The Berry curvature corresponds to the field radiated from a "monopole" with strength σ located at the origin in $\boldsymbol{k}$ space. Then, the equation of motion of the wave-packet center is written as

$$\begin{aligned} \dot{\boldsymbol{r}}_\mathrm{c} &= v\frac{\boldsymbol{k}_\mathrm{c}}{k_\mathrm{c}} + \dot{\boldsymbol{k}}_\mathrm{c} \times \boldsymbol{\Omega}, \\ \dot{\boldsymbol{k}}_\mathrm{c} &= -(\nabla v) k_\mathrm{c}, \end{aligned} \tag{2}$$

where $\boldsymbol{r}_\mathrm{c}$ and $\boldsymbol{k}_\mathrm{c}$ denote the position vector and the wave vector at the wave-packet center. $v = c/n$ is the velocity of light in the media with the refractive index n. The additional term $\dot{\boldsymbol{k}}_\mathrm{c} \times \boldsymbol{\Omega}$ is the anomalous velocity by the Berry curvature, which gives rise to the polarization-dependent Hall effect of light.

The polarization-dependent Hall effect of light is expected to be universal in all wavelengths of electromagnetic waves, which can be also applied to plasma waves in magnetized plasma as anisotropic media. In an electron cyclotron (EC) range of frequencies, a ray-tracing approach has been frequently used for the prediction of a wave-packet motion in fusion plasma. However, the anomalous velocity by the Berry curvature has not been included in conventional ray-tracing codes such as LHDGauss [3] and TRAVIS [4]. The effect of the Berry curvature on propagation of EC waves is of interest because no EC systems in fusion plasma experiments have been designed by including the effect. It may be simple to add the effect of the Berry curvature into the ray-trace equations of the current codes. However, the effect is expected to be significant at cutoffs where the quality of the ray-trace approximation deteriorates due to the wavelength larger than characteristic scale lengths in magnetized plasma. The significance of the effect of the Berry curvature should be naively discussed with the full-wave equations without approximations as a first step, which is the motivation of this paper.

author's e-mail: tsujimura.tohru@nifs.ac.jp

*) This article is based on the presentation at the 29th International Toki Conference on Plasma and Fusion Research (ITC29).

In this paper, the trajectory shift of EC waves due to the Berry curvature was investigated in magnetized plasma. Section 2 describes the introduction of the Berry curvature in magnetized plasma. Results on two-dimensional (2D) full-wave simulations for propagation of EC waves are presented in Section 3. Section 4 summarizes this paper with a future outlook.

2. Berry Curvature in Magnetized Plasma

The Berry curvature in magnetized plasma as anisotropic media is explained in [5]. In this section, the Berry curvature of EC waves propagating in magnetized plasma is briefly introduced. EC waves propagating in magnetized plasma obey the Maxwell equations. Assuming a monochromatic wave in time and space represented with $\exp(\mathrm{i}\boldsymbol{k}\cdot\boldsymbol{r}-\mathrm{i}\omega t)$, where ω and t denote the angular frequency and time, the Maxwell equations are reduced to the eigenvalue problem. Under the cold plasma approximation, the permittivity tensor is written as

$$\begin{aligned}\boldsymbol{\varepsilon}(\omega) &= \varepsilon_0\boldsymbol{\varepsilon}_r(\omega)\\ &= \varepsilon_0\begin{pmatrix} S(\omega) & -\mathrm{i}D(\omega) & 0\\ \mathrm{i}D(\omega) & S(\omega) & 0\\ 0 & 0 & P(\omega)\end{pmatrix},\end{aligned} \tag{3}$$

where the dielectric tensor elements S, D, and P are the same notation of Stix [6]. For this expression, the static magnetic field is in the z direction, i.e., $\boldsymbol{B}_0 = B_0\boldsymbol{e}_z \equiv B_0\boldsymbol{e}_b$, where $\boldsymbol{e}_b$ denotes the unit vector directed in the static magnetic field. Using the eigenvectors of the wave electric field, $\tilde{\boldsymbol{E}}_i$, where i denotes each mode of the EC waves, the Berry connection $\boldsymbol{\Lambda}_i$ and the Berry curvature $\boldsymbol{\Omega}_i$ are obtained by [5]:

$$\begin{aligned}\boldsymbol{\Lambda}_i(\boldsymbol{k}) &= \mathrm{Re}\left[\mathrm{i}\tilde{\boldsymbol{E}}_i^{\dagger}\cdot\frac{\partial}{\partial\omega}\{\omega\boldsymbol{\varepsilon}(\omega)\}\cdot\nabla_{\boldsymbol{k}}\tilde{\boldsymbol{E}}_i\right],\\ \boldsymbol{\Omega}_i(\boldsymbol{k}) &= \nabla_{\boldsymbol{k}}\times\boldsymbol{\Lambda}_i(\boldsymbol{k}),\end{aligned}$$

where the symbol † means complex conjugate operation. Thus, the direction of the anomalous velocity affecting the wave packet of the EC wave is obtained by $\dot{\boldsymbol{k}}_{\mathrm{c}}\times\boldsymbol{\Omega}_i$.

For the EC waves propagating parallel to the static magnetic field, i.e., $\boldsymbol{k}\parallel\boldsymbol{B}_0$, the eigenvectors of the electric field are $\tilde{\boldsymbol{E}}_{\mathrm{R,L}} = \boldsymbol{e}_x \pm \mathrm{i}\boldsymbol{e}_y$, which are the right-handed (R) wave and the left-handed (L) wave. Therefore, there is no Berry phase effect [5]. For the EC waves propagating perpendicular to the static magnetic field, i.e., $\boldsymbol{k}\perp\boldsymbol{B}_0$, there are two eigenmodes, i.e., the ordinary (O) wave and the extraordinary (X) wave. The eigenvector of the O wave is $\tilde{\boldsymbol{E}}_{\mathrm{O}} = \boldsymbol{e}_z$. Therefore, there is no Berry phase effect [5]. On the other hand, the eigenvector of the X wave is

$$\tilde{\boldsymbol{E}}_{\mathrm{X}} = \frac{1}{\omega}\boldsymbol{\varepsilon}_r^{-1}\cdot(\boldsymbol{e}_z\times\boldsymbol{k}),$$

with the dispersion relation

$$n_{\mathrm{X}}^2 = \frac{c^2(k_x^2+k_y^2)}{\omega^2} = \frac{RL}{S}. \tag{4}$$

The eigenvector is complex-valued due to the permittivity tensor, giving rise to nontrivial Berry properties. Thus, the Berry curvature is obtained by [5]:

$$\boldsymbol{\Omega}_{\mathrm{X}} = \gamma\frac{\boldsymbol{e}_b}{k^2}, \tag{5}$$

where

$$\begin{aligned}\gamma &\equiv \frac{\mathrm{Re}\left[\mathrm{i}\left\{4\alpha_1\alpha_2\beta_1 + 2\left(|\alpha_1|^2+|\alpha_2|^2\right)\beta_2\right\}\right]}{(|\alpha_1|^2+|\alpha_2|^2)\beta_1 - 2\alpha_1\alpha_2\beta_2},\\ \alpha_1 &\equiv \frac{S}{RL},\quad \alpha_2 \equiv \frac{\mathrm{i}D}{RL},\\ \beta_1 &\equiv \frac{\partial}{\partial\omega}(\omega\varepsilon_0 S),\quad \beta_2 \equiv \frac{\partial}{\partial\omega}(\omega\varepsilon_0 D).\end{aligned}$$

For the X wave, there are two "monopoles" at the right-hand cutoff and the left-hand cutoff, where $k = 0$. Figure 1 shows an example of the Berry curvature of the X wave along with the squared refractive index as a function of $\omega_{\mathrm{pe}}^2/\omega^2 \propto n_{\mathrm{e}}$, where ω_{pe} and n_{e} denote the angular plasma frequency for electrons and the electron density. In these calculations, the static magnetic field strength B_0 is

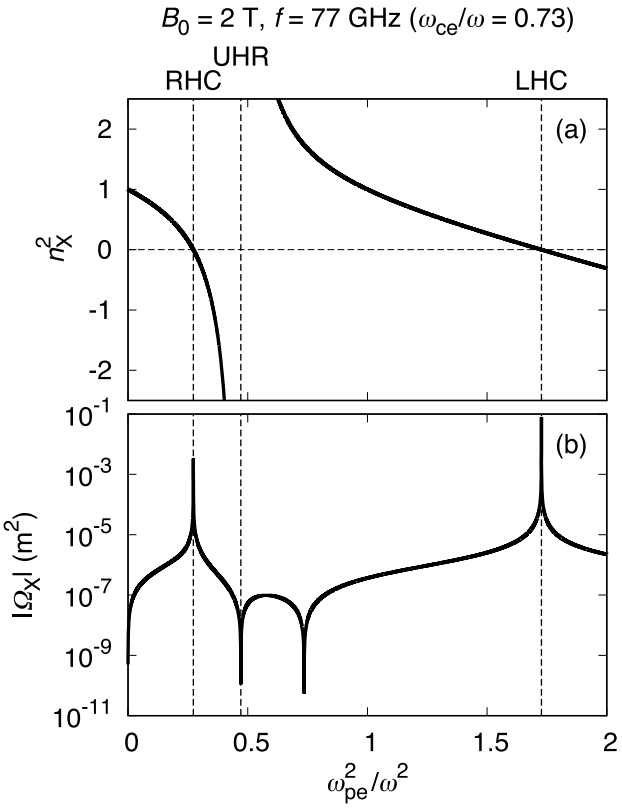

Fig. 1 (a) The squared refractive index and (b) the absolute value of the Berry curvature for the X wave as a function of $\omega_{\mathrm{pe}}^2/\omega^2$. "RHC", "UHR", and "LHC" denote right-hand cutoff, upper hybrid resonance, and left-hand cutoff.

set 2 T for $f = 77$ GHz [7], thus $\omega_{ce}/\omega = 0.73$, where ω_{ce} denotes the angular EC frequency. It is clearly seen that the Berry curvature is strongly enhanced at the right-hand and the left-hand cutoffs. This result indicates that the transverse shift of the center of the reflected wave packet is expected at those cutoffs. The anomalous velocity is directed in $\nabla n_X \times \boldsymbol{e}_b$, which indicates that the transverse shift occurs at those cutoffs in the direction perpendicular not only to the gradient of the refractive index but also to the static magnetic field.

3. Transverse Shift in Propagation of EC Waves

The transverse shift in propagation of EC waves is numerically investigated with 2D simulations performed by the commercial FEM (finite element method) software, COMSOL Multiphysics with its RF solver [8–11]. The simulations are restricted in 2D due to limited computational resources. The simulation area is set to be a rectangular with a width of 50 mm and a height of 100 mm. Figure 2 shows the n_e profile. The n_e profile is defined as

$$\begin{aligned} n_e(x,y) &= n_{e0} \exp\left\{\frac{u(x,y) - W_0}{L_0}\right\}, \\ u(x,y) &= W_0 + \frac{1}{\sqrt{2}}\left(x - \frac{W_0}{2}\right) + \frac{y}{\sqrt{2}}, \end{aligned} \tag{6}$$

where $n_{e0} = 4.82 \times 10^{19}$ m^{-3}, $W_0 = 50$ mm, and $L_0 = 20$ mm for 45° of incidence and reflection. Thus, the right-hand cutoff layer is located at $y \approx -x$. The wave frequency f is set at 77 GHz. For simplicity, the static magnetic field B_0 is uniformly set at 2 T and its direction is varied for each simulation run. Thus, the gradient of the refractive index is

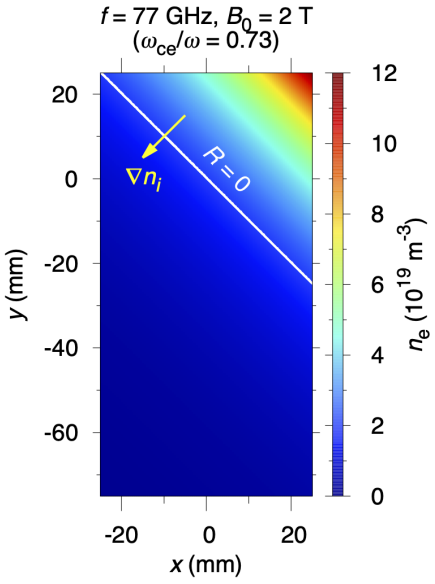

Fig. 2 n_e profile along with the right-hand cutoff layer where $R = 0$. The direction of the gradient of the refractive index ∇n_i for each mode is shown by an arrow.

directed to the gradient of the electron density. The wave electric field in a form of the Gaussian beam is excited at the line of $x = -25$ mm (the boundary at the left side), given by

$$\begin{aligned} &E(x,y) \\ &\quad = E_0 \frac{w_0}{w(x)} \exp\left[-\frac{y^2}{w(x)^2} + \mathrm{i}\left\{-k_0 \frac{y^2}{2R(x)} + \zeta(x)\right\}\right] \\ &\quad \text{at } x = -25 \text{ mm}, \end{aligned} \tag{7}$$

where

$$w(x) = w_0 \sqrt{1 + \left(\frac{x}{x_R}\right)^2}, \quad x_R = \frac{\pi w_0^2}{\lambda_0},$$
$$R(x) = x\left\{1 + \left(\frac{x_R}{x}\right)^2\right\}, \quad \zeta(x) = \tan^{-1}\frac{x}{x_R}.$$

Here, k_0 and λ_0 are the wavenumber and the wavelength in the vacuum. The focal length x_R is set at 25 mm and the beam waist w_0 becomes 5.6 mm in the vacuum. The incident polarization, i.e., the direction of the excited electric field, is varied for each simulation run. The size of triangular meshes is 0.2 mm at a maximum and 0.02 mm at a minimum. Propagation of the excited wave is calculated by solving the telegraphic equation given by

$$\nabla \times (\nabla \times \boldsymbol{E}) - k_0^2 \boldsymbol{\varepsilon}_r \cdot \boldsymbol{E} = \boldsymbol{0},$$

where the cold plasma dielectric tensor $\boldsymbol{\varepsilon}_r$ given in Eq. (3) includes the effect of collisions with the artificial collision frequency of $\nu_0 = 10^{-3}\omega$ [12, 13]. This effect simply prevents numerical divergence at the upper hybrid resonance where resonant waves should be collisionally damped. The scattering boundary condition is applied to prevent reflection at the simulation boundaries.

When the static magnetic field is in the $\pm z$ direction, the anomalous velocity for the X wave is in the $\mp \boldsymbol{e}_x \pm \boldsymbol{e}_y$ directions, parallel to the reflection line at the right-hand cutoff. Thus, the transverse shift can be observed even in 2D simulations. In this case, the y-directed linearly-polarized electric field given by Eq. (7) is excited as the X wave. Figure 3 shows the electric field strength in the X wave propagation. The incident X wave with the shape of the Gaussian beam is reflected at the right-hand cutoff layer. The transverse shift occurs at the layer during reflection. The direction of the transverse shift depends on the direction of the static magnetic field. The existence of the transverse shift is recognizable by changing the magnetic field polarity. In terms of photons, the generated transverse shift means that orbital angular momenta are generated in the z direction, i.e., the direction of $(\mp \boldsymbol{e}_x \pm \boldsymbol{e}_y) \times \boldsymbol{k}$, although there is no spin angular momentum in the $\boldsymbol{k}$ direction for the linearly-polarized incident X wave. The difference of the transverse shift due to the magnetic field polarity is shown in Fig. 4. The difference between each peak position of the reflected electric field strength profile is observed to

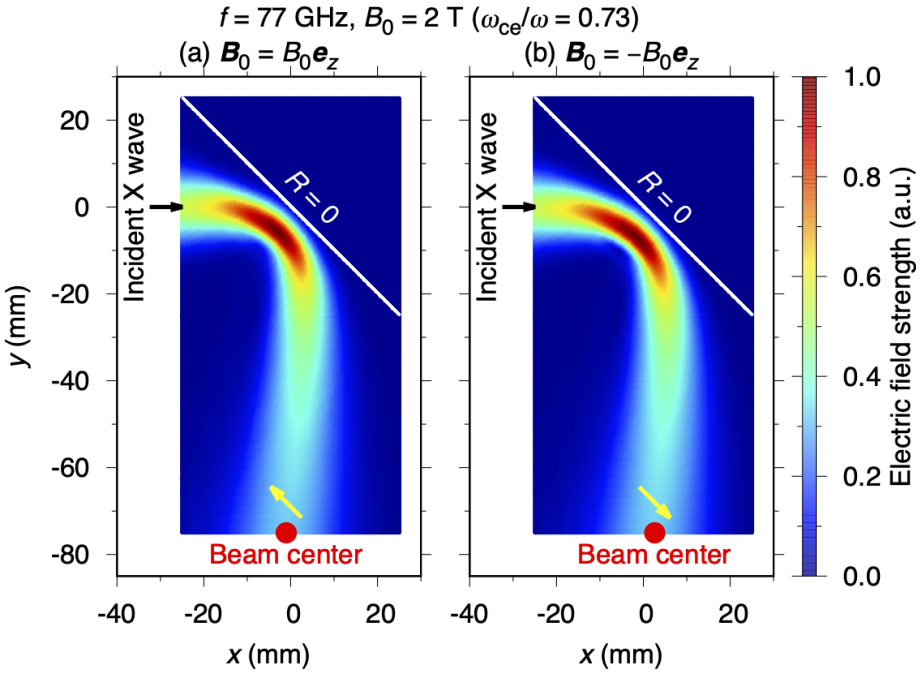

Fig. 3 Electric field strength for the X wave in the cases of (a) $\boldsymbol{B}_0 = B_0\boldsymbol{e}_z$ and (b) $\boldsymbol{B}_0 = -B_0\boldsymbol{e}_z$.

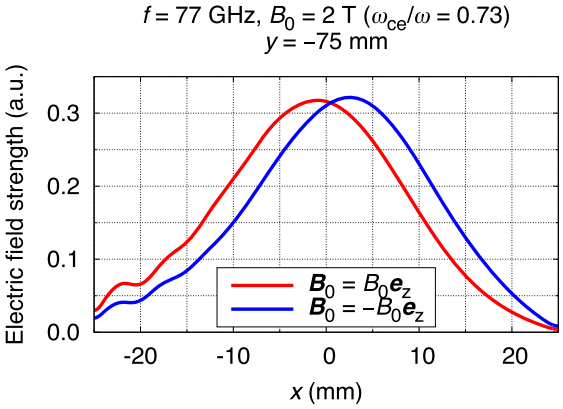

Fig. 4 Electric field strength at $y = -75$ mm (the boundary at the bottom side) as a function of x for the X wave in the cases of $\boldsymbol{B}_0 = \pm B_0\boldsymbol{e}_z$.

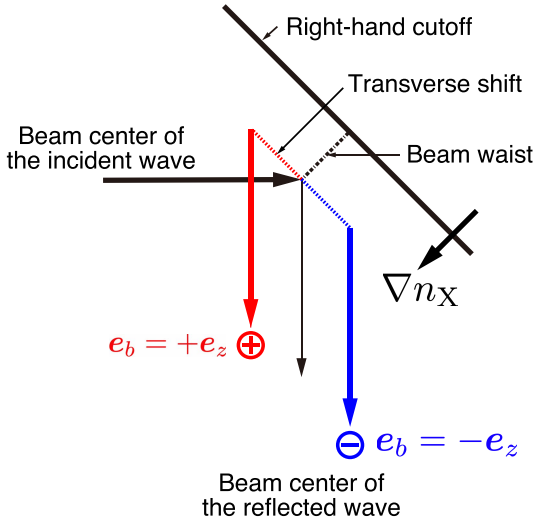

Fig. 5 Schematic diagram of the transverse shift for the X wave in the cases of $\boldsymbol{e}_b = \pm\boldsymbol{e}_z$.

be 3.6 mm, which is comparable to the wavelength in the vacuum. For simplicity, suppose that the trajectory of the wave is straight and reflection is at a right angle, as shown in Fig. 5. Using Eqs. (2), (4), (5), and (6), the transverse shift δ of the beam center can be estimated to be

$$\begin{aligned}\delta &\approx \frac{4\sqrt{2}\pi}{\lambda_0}\left|\int_{u_i}^{u_r}\frac{\mathrm{d}n_\mathrm{X}}{\mathrm{d}u}\Omega_\mathrm{X}\mathrm{d}u\right| \\ &= \frac{\sqrt{2}}{\pi}\lambda_0\left|\int_{u_i}^{u_r}\frac{\mathrm{d}n_\mathrm{X}}{\mathrm{d}u}\frac{\gamma}{n_\mathrm{X}^2}\mathrm{d}u\right|,\end{aligned} \tag{8}$$

where u_i and u_r denote the position of the incident wave excited and the reflection position. It is noted that the beam center is not reflected exactly at the right-hand cutoff layer but reflected in front of the layer, so that the distance between the reflection point and the right-hand cutoff layer is approximated as the beam waist w_0. Due to the finite beam size, the beam center cannot be affected by the diverging Berry curvature at the right-hand cutoff, which limits the transverse shift to a finite length. Then, the difference of the transverse shift between the two cases with $\boldsymbol{e}_b = \pm\boldsymbol{e}_z$ is estimated to be $2\delta \approx 0.75\lambda_0 \approx 2.9$ mm, which is the same order as obtained from Fig. 4. In isotropic media, γ is replaced with constant $\sigma = [-1, 1]$ given by Eq. (1), so that the integral in Eq. (8) shows the change of the reciprocal of the refractive index. The transverse shift is restricted to

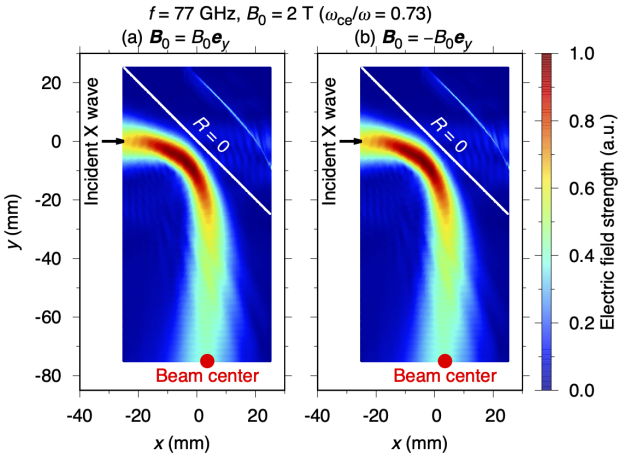

Fig. 6 Electric field strength in the cases of (a) $\boldsymbol{B}_0 = B_0\boldsymbol{e}_y$ and (b) $\boldsymbol{B}_0 = -B_0\boldsymbol{e}_y$. The z-directed linearly polarized wave is excited to couple to the X wave.

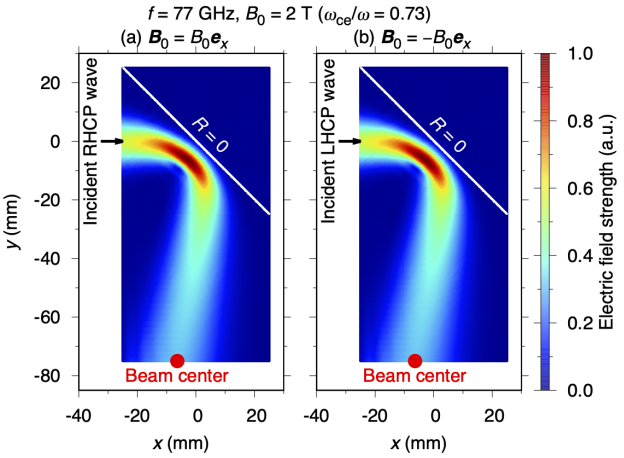

Fig. 7 Electric field strength in the cases of (a) $\boldsymbol{B}_0 = B_0\boldsymbol{e}_x$ and (b) $\boldsymbol{B}_0 = -B_0\boldsymbol{e}_x$. The right-handed circularly polarized (RHCP) wave for (a) and the left-handed circularly polarized (LHCP) wave for (b) are excited, respectively, to couple to the R wave.

the order of the wavelength in the vacuum due to the spin angular momentum. In the case of the X wave, γ changes from 0 at the vacuum to 2 at the right-hand cutoff, so that the integral in Eq. (8) shows the same order as in the case of the isotropic media. At that time, the transverse shift is also restricted to the order of the wavelength in the vacuum.

On the other hand, when the static magnetic field is in the $\pm y$ direction, the anomalous velocity for the X wave is in the $\mp\boldsymbol{e}_z$ directions, perpendicular to the x-y plane. In this case, the transverse shift cannot be observed in 2D simulations. The simulation results are shown in Fig. 6, which indicates that there is no difference in the electric field strength between the cases of $\boldsymbol{B}_0 = \pm B_0\boldsymbol{e}_y$. The transverse shift can be expected in the z direction only when simulations are performed in 3D.

For the R wave, there can be no Berry phase effect. When the static magnetic field is in the $\pm x$ direction, the incident polarization should be the right-handed circular polarization for $\boldsymbol{e}_b = \boldsymbol{e}_x$ or the left-handed circular polarization for $\boldsymbol{e}_b = -\boldsymbol{e}_x$, so that the incident wave can couple to the R wave in the magnetized plasma. The simulation results are shown in Fig. 7, which indicates that there is no difference in the electric field strength between the two cases. The reflected wave almost becomes the X wave due to $\boldsymbol{k} \perp \boldsymbol{e}_x$. However, the anomalous velocity is directed in the $\pm\boldsymbol{e}_z$ directions. Thus, the trajectory shift is not observed in 2D.

As a supplement, the incident R wave shown in Fig. 7 is refracted more than the incident X wave shown in Fig. 6 during reflection at the right-hand cutoff layer. The incident R wave almost becomes the X wave during reflection. The incident X wave almost becomes a mixture of the R wave and the L wave during reflection. Since the wavelength of the X wave is shorter than that of the R wave, the effect of refraction is stronger in the case shown in Fig. 7. However, the difference of the wave trajectories is not related to the transverse shift due to the Berry curvature discussed in this paper.

4. Summary and Outlook

The polarization-dependent Hall effect of light was investigated for propagation of EC waves in magnetized plasma. According to the Berry curvature calculated for the modes in the cases of parallel propagation and perpendicular propagation, full-wave simulations were performed in 2D space, where the incident EC waves were reflected at the right-hand cutoff layer in the varied electron density profile for various directions of the static magnetic field. The observed transverse shift in the X wave propagation was comparable to the wavelength in the vacuum.

In this paper, only the polarization-dependent Hall effect of light was discussed. Light has not only spin angular momentum but also orbital angular momentum by adding $\exp(\mathrm{i}l\varphi)$ to the phase term, which is a so-called optical vortex, where l is the topological charge and φ is the azimuthal angle around the propagation axis of the beam. It is known that the Berry curvature produced by the orbital angular momentum in the optical vortex is added to the Berry curvature produced by the polarization-dependent spin angular momentum in isotropic media [14]. The important point is that $|l|$ can be larger than $|\sigma|$ (≤ 1). Thus, the transverse shift can be larger than the order of the wavelength. This phenomenon is also expected for propagation of vortex EC waves in magnetized plasma.

Acknowledgments

This work was supported in part by JSPS KAKENHI Grant Number JP19K14687 and by the NINS program for cross-disciplinary study (Grant Number 01311802).

[1] M. Onoda *et al.*, Phys. Rev. Lett. **93**, 083901 (2004).
[2] M.V. Berry, Proc. R. Soc. Lond. A **392**, 45 (1984).
[3] T.I. Tsujimura *et al.*, Nucl. Fusion **55**, 123019 (2015).
[4] N.B. Marushchenko *et al.*, Comput. Phys. Commun. **185**, 165 (2014).
[5] S.A.H. Gangaraj *et al.*, IEEE J. Multiscale Multiphys. Comput. Tech. **2**, 3 (2017).
[6] T.H. Stix, *Waves in Plasmas* (American Institute of Physics, New York, 1992).
[7] T.I. Tsujimura *et al.*, Fusion Eng. Des. **153**, 111480 (2020).
[8] https://www.comsol.com
[9] T. Mori *et al.*, Plasma Fusion Res. **14**, 3401134 (2019).
[10] S. Shiraiwa *et al.*, Phys. Plasma **17**, 056119 (2010).
[11] C. Lau *et al.*, Plasma Phys. Control. Fusion **61**, 045008 (2019).
[12] D.G. Swanson, *Plasma Waves, 2nd Edition* (Institute of Physics Publishing, Bristol and Philadelphia, 2003).
[13] T. Yamamoto *et al.*, Plasma Fusion Res. **3**, S1075 (2008).
[14] K.Y. Bliokh, Phys. Rev. Lett. **97**, 043901 (2006).